The top quark electro-weak couplings after LHC Run 2

V. Miralles[a], M. Miralles López[a], M. Moreno Llácer[a], A. Peñuelas[a,b], M. Perelló[a], M. Vos[a]

[a]IFIC, Universitat de València and CSIC, [b]U. Mainz, Prisma

Based on arXiv:2107.13917

Introduction

- Being the heaviest particle of the SM the **top-quark** is a good candidate for searching for **new physics**
- Its EW couplings are specially relevant in many extensions of the SM
- As the top-quark was not produced in LEP its EW sector could not be precisely measured until now
- The LHC data allows, finally, for **precise measurements of this sector**
- Here we present results of a global fit to top-quark EW couplings
- We used the most recent available data from the LHC (**ATLAS** and **CMS**), and also from **LEP** and **Tevatron**
- We include the **QCD corrections at NLO** on most of the observables used and the latest $pp \to t\bar{t}Z$ and $pp \to t\bar{t}\gamma$ **differential cross-sections**
- The fits have been performed using HEPfit [1910.14012]

Theoretical Framework

- We use an **EFT description** to parametrise deviations from the SM

$$\mathscr{L}_{\text{eff}} = \mathscr{L}_{\text{SM}} + \frac{1}{\Lambda^2}\sum_i C_i O_i + \mathscr{O}\left(\Lambda^{-4}\right)$$

- The Wilson coefficients can be interpreted in terms of NP mediators
- We include Λ^{-2} terms from the **interference between the SM and D6**
- We also include Λ^{-4} terms arising from **squaring the D6**

Both fits are presented

- The effects of D8 operators, contributing to the same Λ^{-4} order, are omitted

$$\sigma = \sigma_{\text{SM}} + \underbrace{\frac{1}{\Lambda^2}\sum C_i O_i}_{\text{SM }\times\text{D6}} + \underbrace{\left(\frac{1}{\Lambda^2}\sum C_i O_i\right)\left(\frac{1}{\Lambda^2}\sum C_j O_j\right)}_{\text{D6}\times\text{D6}} + \underbrace{O(1/\Lambda^4)}_{\text{SM }\times\text{D8}}$$

- We only consider the **EW two-fermion operators** and ignore imaginary parts
- The four-fermion operators are ignored

EW top-quark EFT Basis

Left and right-handed couplings of the t- and b-quark to the Z

$$O^3_{\varphi Q} \equiv \frac{1}{2}(\bar{q}\tau^I\gamma^\mu q)\left(\varphi^\dagger i\overleftrightarrow{D}^I_\mu \varphi\right)$$
$$O^1_{\varphi Q} \equiv \frac{1}{2}(\bar{q}\gamma^\mu q)\left(\varphi^\dagger i\overleftrightarrow{D}_\mu \varphi\right)$$
$$O_{\varphi u} \equiv \frac{1}{2}(\bar{u}\gamma^\mu u)\left(\varphi^\dagger i\overleftrightarrow{D}_\mu \varphi\right)$$
$$O_{\varphi d} \equiv \frac{1}{2}(\bar{d}\gamma^\mu d)\left(\varphi^\dagger i\overleftrightarrow{D}_\mu \varphi\right)$$

EW dipole operators

$$O_{uW} \equiv (\bar{q}\tau^I\sigma^{\mu\nu}u)\left(\varepsilon\varphi^* W^I_{\mu\nu}\right)$$
$$O_{dW} \equiv (\bar{q}\tau^I\sigma^{\mu\nu}d)\left(\varphi W^I_{\mu\nu}\right)$$
$$O_{uB} \equiv (\bar{q}\sigma^{\mu\nu}u)(\varepsilon\varphi^* B_{\mu\nu})$$
$$O_{dB} \equiv (\bar{q}\sigma^{\mu\nu}d)(\varphi B_{\mu\nu})$$

Chromo magnetic dipole operators

$$O_{uG} \equiv (\bar{q}\sigma^{\mu\nu}T^A u)\left(\varepsilon\varphi^* G^A_{\mu\nu}\right)$$
$$O_{dG} \equiv (\bar{q}\sigma^{\mu\nu}T^A d)\left(\varphi G^A_{\mu\nu}\right)$$

Top/Bottom yukawa

$$O_{u\varphi} \equiv (\bar{q}u)(\varepsilon\varphi^*\ \varphi^\dagger\varphi)$$
$$O_{d\varphi} \equiv (\bar{q}d)(\varphi\ \varphi^\dagger\varphi)$$

Charged current interaction

$$O_{\varphi ud} \equiv \frac{1}{2}(\bar{u}\gamma^\mu d)(\varphi^T\varepsilon i D_\mu\varphi)$$

- Rotation of Warsaw basis following [1802.07237] (LHC Top WG)

$$O^1_{\varphi Q} \to O^-_{\varphi Q} = O^1_{\varphi Q} - O^3_{\varphi Q}; \qquad O_{xB} \to O_{xZ} = -\sin\theta_W O_{xB} + \cos\theta_W O_{xW}$$

- We make use of the **Warsaw Basis**

$$C^-_{\varphi Q},\ C^{(3)}_{\varphi Q},\ C_{\varphi t},\ C_{tW},\ C_{tZ},\ C_{t\varphi},\ C_{\varphi tb},\ C_{bW}$$
$$C_{\varphi b} \qquad C_{bZ}$$

- **Linear Fit** Λ^{-2} : 7 d.o.f.
- **Quadratic Fit** $\Lambda^{-2} + \Lambda^{-4}$: 10 d.o.f.
- **Operators for these coefficients** are included in the fit but limits are not reported since they are not competitive

Methods & Data

- Dependence of the observables calculated at NLO in QCD with the **Monte Carlo generator MG5_aMC@NLO** [JHEP 07 (2014) 079]
- **SMEFT@NLO** [arXiv:2008.11743] UFO model was used except for C_{bW} , $C_{\varphi tb}$, C_{bZ} and $C_{\varphi b}$ where the **TEFT_EW** [JHEP 05 (2016) 052] UFO model was used
- The fit is performed as a Bayesian statistical analysis of the model using the open source **HEPfit** [1910.14012]

Process	Observable	$\sqrt{s}$	$\int \mathcal{L}$	Experiment
$pp \to t\bar{t}H + tHq$	σ	13 TeV	140 fb^{-1}	ATLAS
$pp \to t\bar{t}Z$	$d\sigma/dp_T^Z$ (7 bins)	13 TeV	140 fb^{-1}	ATLAS
$pp \to t\bar{t}\gamma$	$d\sigma/dp_T^\gamma$ (11 bins)	13 TeV	140 fb^{-1}	ATLAS
$pp \to tZq$	σ	13 TeV	77.4 fb^{-1}	CMS
$pp \to t\gamma q$	σ	13 TeV	36 fb^{-1}	CMS
$pp \to t\bar{t}W$	σ	13 TeV	36 fb^{-1}	CMS
$pp \to t\bar{b}$ (s-ch)	σ	8 TeV	20 fb^{-1}	LHC
$pp \to tW$	σ	8 TeV	20 fb^{-1}	LHC
$pp \to tq$ (t-ch)	σ	8 TeV	20 fb^{-1}	LHC
$t \to Wb$	F_0, F_L	8 TeV	20 fb^{-1}	LHC
$p\bar{p} \to t\bar{b}$ (s-ch)	σ	1.96 TeV	9.7 fb^{-1}	Tevatron
$e^-e^+ \to b\bar{b}$	R_b , A_{FBLR}^{bb}	$\sim$ 91 GeV	202.1 pb^{-1}	LEP/SLD

SM fit

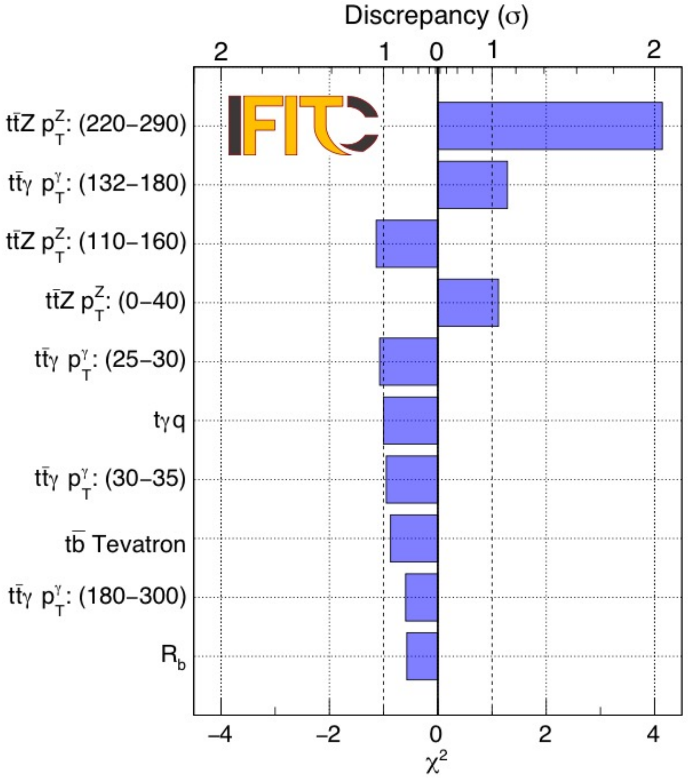

EFT fits

In both fits, published correlations between differential p_T bins, LEP observables and W helicity fractions have been included

Fit	$\chi^2/d.o.f.$	p-value
SM	21.3/29	0.85
EFT Lin.	21.5/22	0.49
EFT Quad.	20.1/19	0.39

Sensitivity

$$\sigma = \sigma_{SM} + \sum_i \frac{\mathcal{C}_i}{\Lambda^2}\sigma_i^{(1)} + \sum_{ij} \frac{\mathcal{C}_i\mathcal{C}_j}{\Lambda^4}\sigma_{ij}^{(2)} + \mathcal{O}\left(\Lambda^{-4}\right)$$

- The observables and coefficients in **red** are not included
- The $pp \to t\bar{t}$ process is omitted in the fit in order to be consistent as it is used to reduce the dependence of $pp \to t\bar{t}X$ on Wilson coefficients that have not been included.

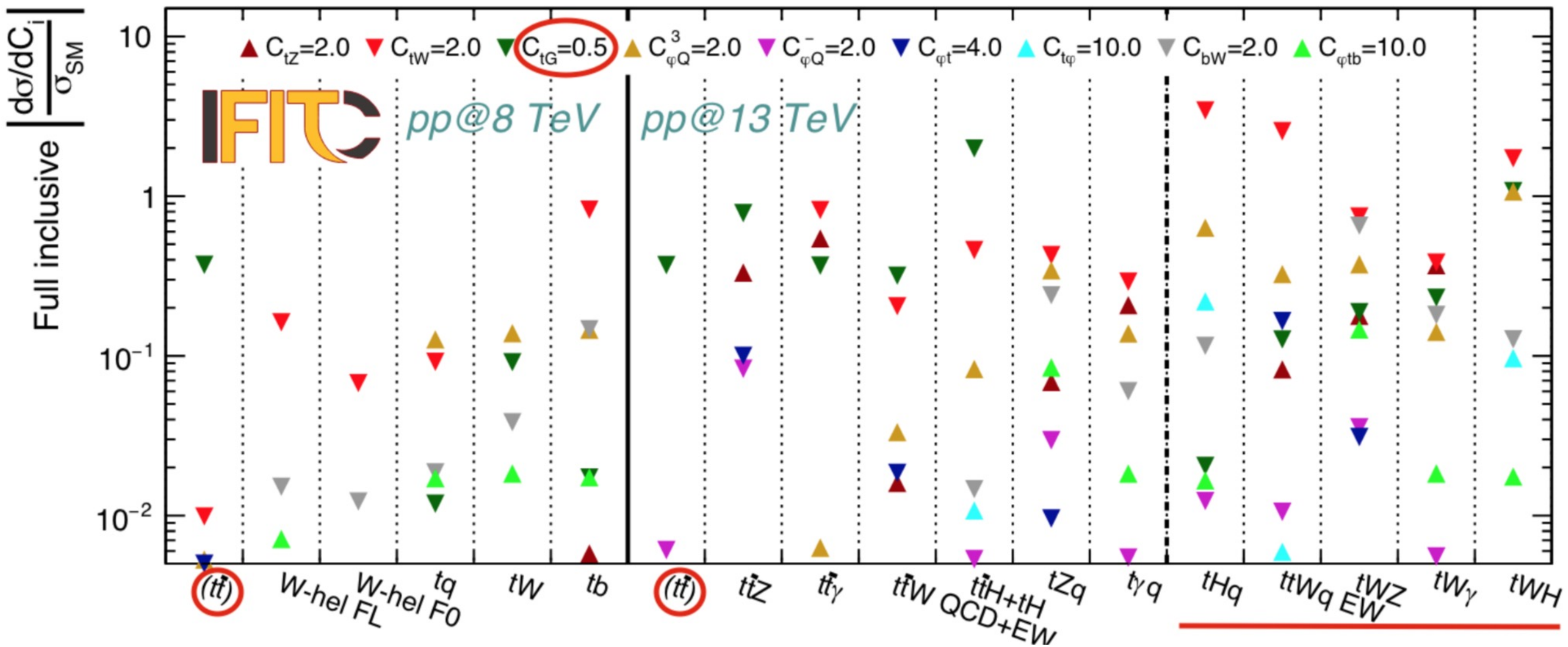

Results – Sensitivity Individual Constraints

- **Good interplay** between the parameters and chosen observables
- The **differential** cross sections (darker regions) provide the **best constraints** for some observables

Individual 95% probability bounds including Λ^{-4} terms

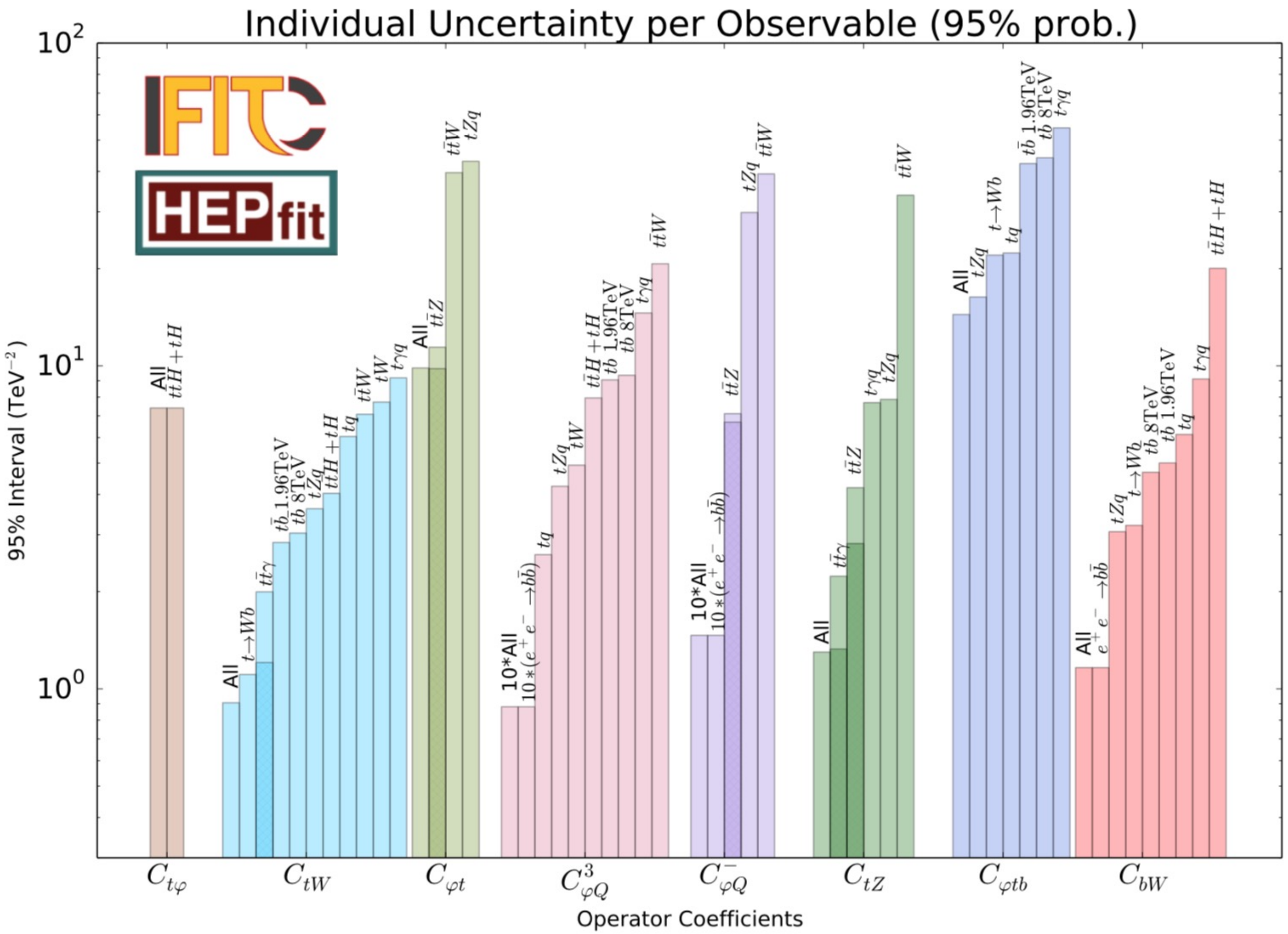

Differential measurements are indicated as darker bars

Results – Complementarity btw. Observables

- Very **good complementarity** between the observables
- The **global fit** marginalised limit is quite close to the intersection of individual fits. The data set is diverse enough to **avoid the existence of blind directions**
- Watch out for: LEP in $C_{\varphi Q}^{-}, C_{\varphi Q}^{(3)}$; $t\bar{t}Z$ in C_{tZ}; $t\bar{t}\gamma$ and Whel. in C_{tW}

2D 95% probability contours including Λ^{-4} terms

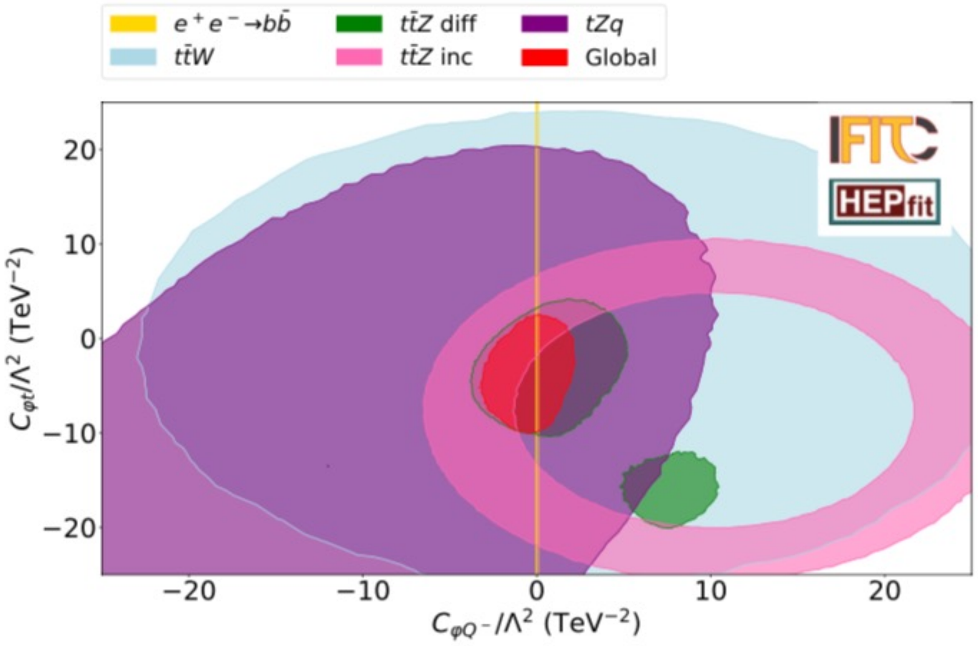

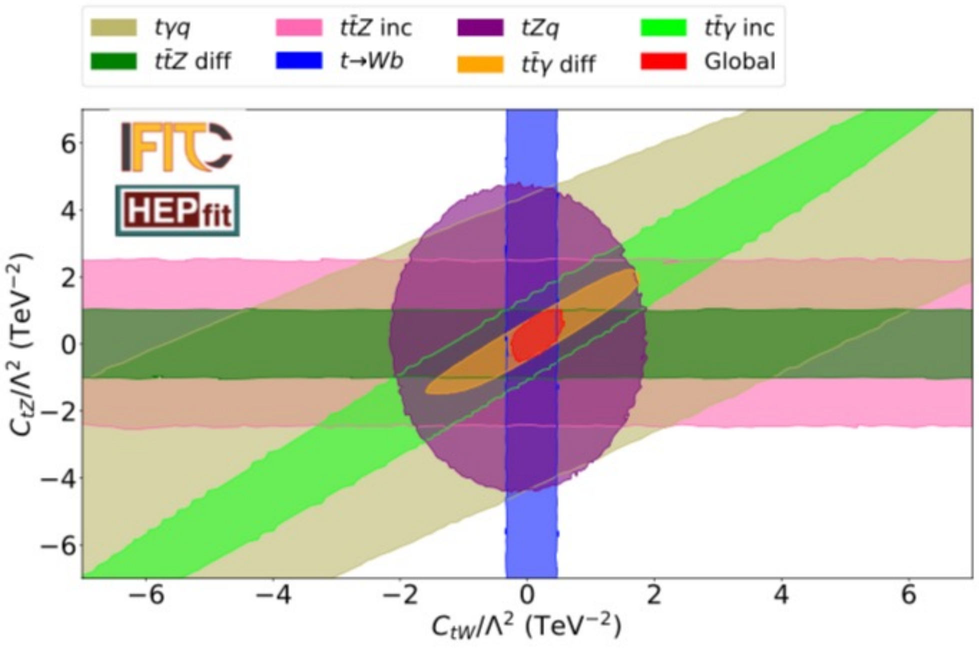

Results – Global Fit

- The **constrains** of the linear (Λ^{-2}) global fit are similar to those of the quadratic (Λ^{-2} + Λ^{-4} terms) global fit for most cases
- Estimation of the impact of correlations between the observables and the **extension** of our basis with **7 four-fermion** operators $C^{8}_{tu}, C^{8}_{td}, C^{1,8}_{Qq}, C^{3,8}_{Qq}, C^{8}_{Qu}, C^{8}_{Qd}, C^{8}_{tq},$ and C_{tG}
- **Robust Limit**: Envelope found from combining all the results
  - Effect of the 8 additional operators + $pp \to t\bar{t}$ at 13 TeV and Tevatron
  - Correlations between different observables (ansatz of non-published correlations has been estimated)
  - MC theory scale uncertainties in EFT parametrisations (max. 5% effect)

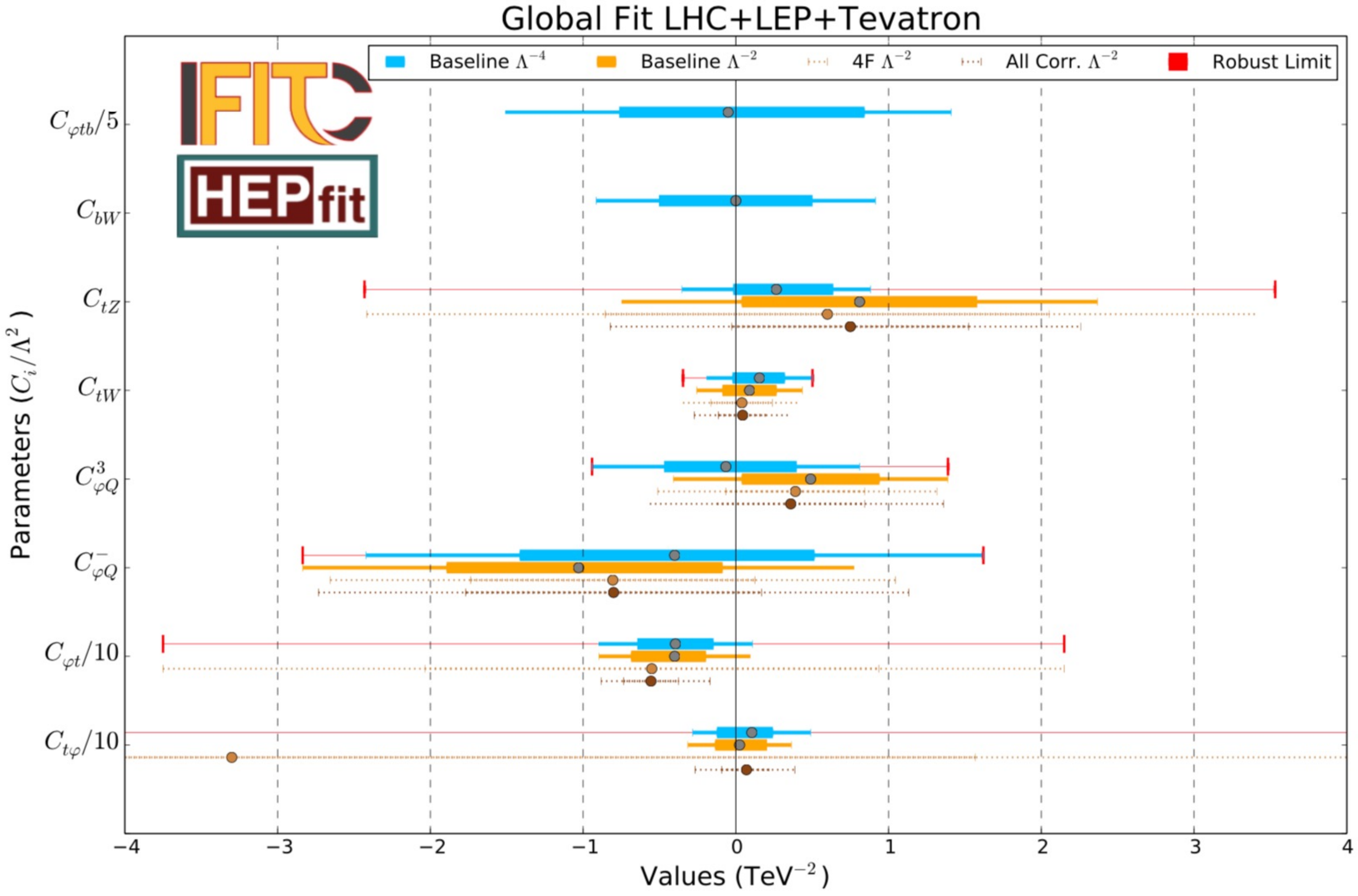

Compatibility with 0 within 2σ and 95% probability bounds $\pm$ 0.35 to ± 8 TeV^{-2}

Future Colliders – Prospects

HL-LHC error reduction

Theoretical Uncertainties		⟶	scale with 1/2
Experimental Uncertainties	Modelling	⟶	scale with 1/2
	Systematic	⟶	scale with $1/\sqrt{\mathscr{L}}$
	Statistical	⟶	scale with $1/\sqrt{\mathscr{L}}$

Results from [JHEP12(2019)098] show the extraordinary impact of adding the data from a e^+e^- collider working at 500 GeV → It is crucial to go $\sqrt{s} > 2m_t$

Expected improvement for each observable
Dark: individual Light: global

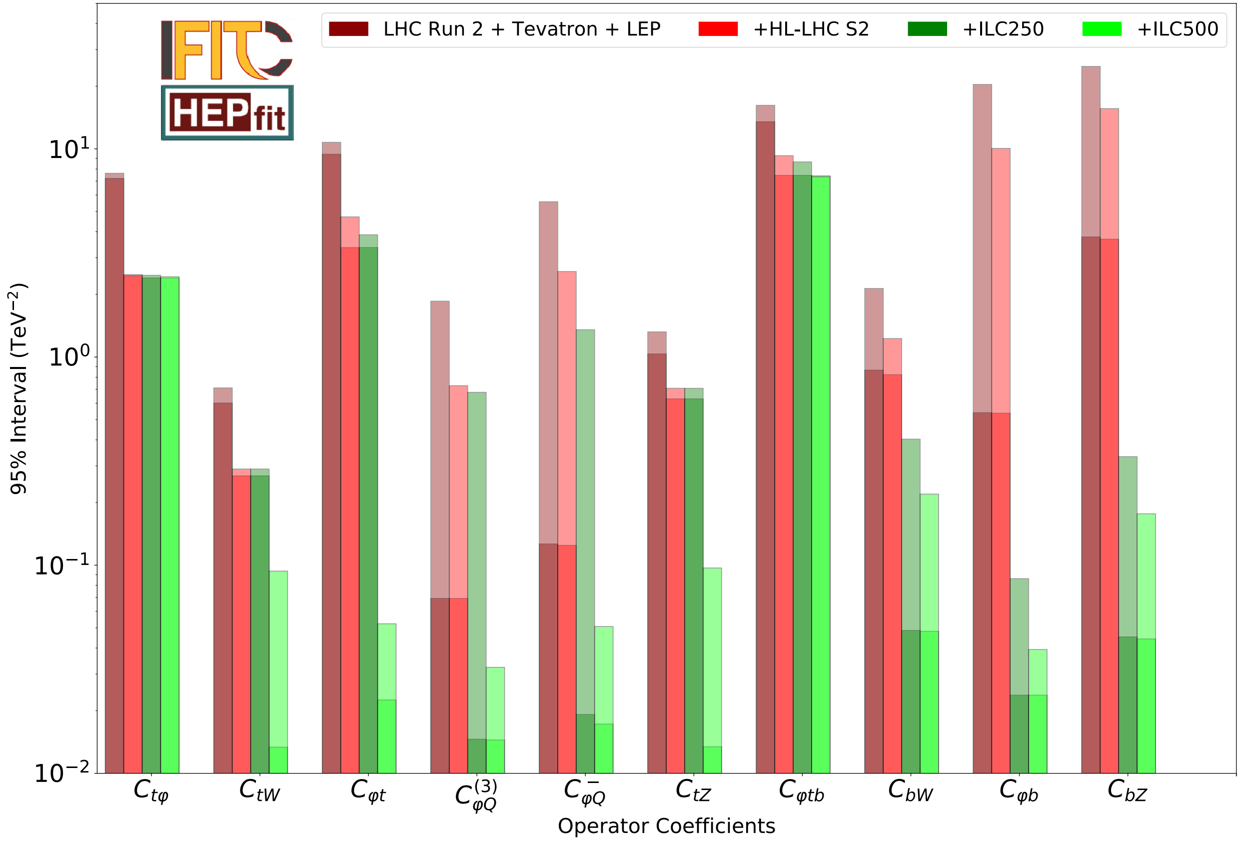

Conclusions

- All the results are **compatible with the SM** with a 95% probability
- We find a **reduction** of the uncertainty of all the parameters of around a **factor two** with respect to our previous work [JHEP12(2019)098]
- **LEP measurements** provide tight bounds on several operators as the left-handed coupling $C_{\varphi Q}^{-}$ and $C_{\varphi Q}^{(3)}$
- The addition of the **differential cross sections** of $pp \to t\bar{t}Z$ and $pp \to t\bar{t}\gamma$ have an important effect on C_{tZ} and $C_{\varphi t}$
- The limits are quite **robust** even when we only consider linear terms, except for C_{bW} , $C_{\varphi tb}$, and C_{tZ}
- Adding important correlations between the observables does not dramatically change the results, but increasing the basis has an effect
- We find **the most stringent bound on top EW couplings** from an EFT including all relevant 2-fermions degrees of freedom (see [JHEP 04 (2019) 100], [JHEP 02 (2020) 131], [CMS-PAS-TOP-19-001])

BACKUP

Results – Differential Cross Section Effect

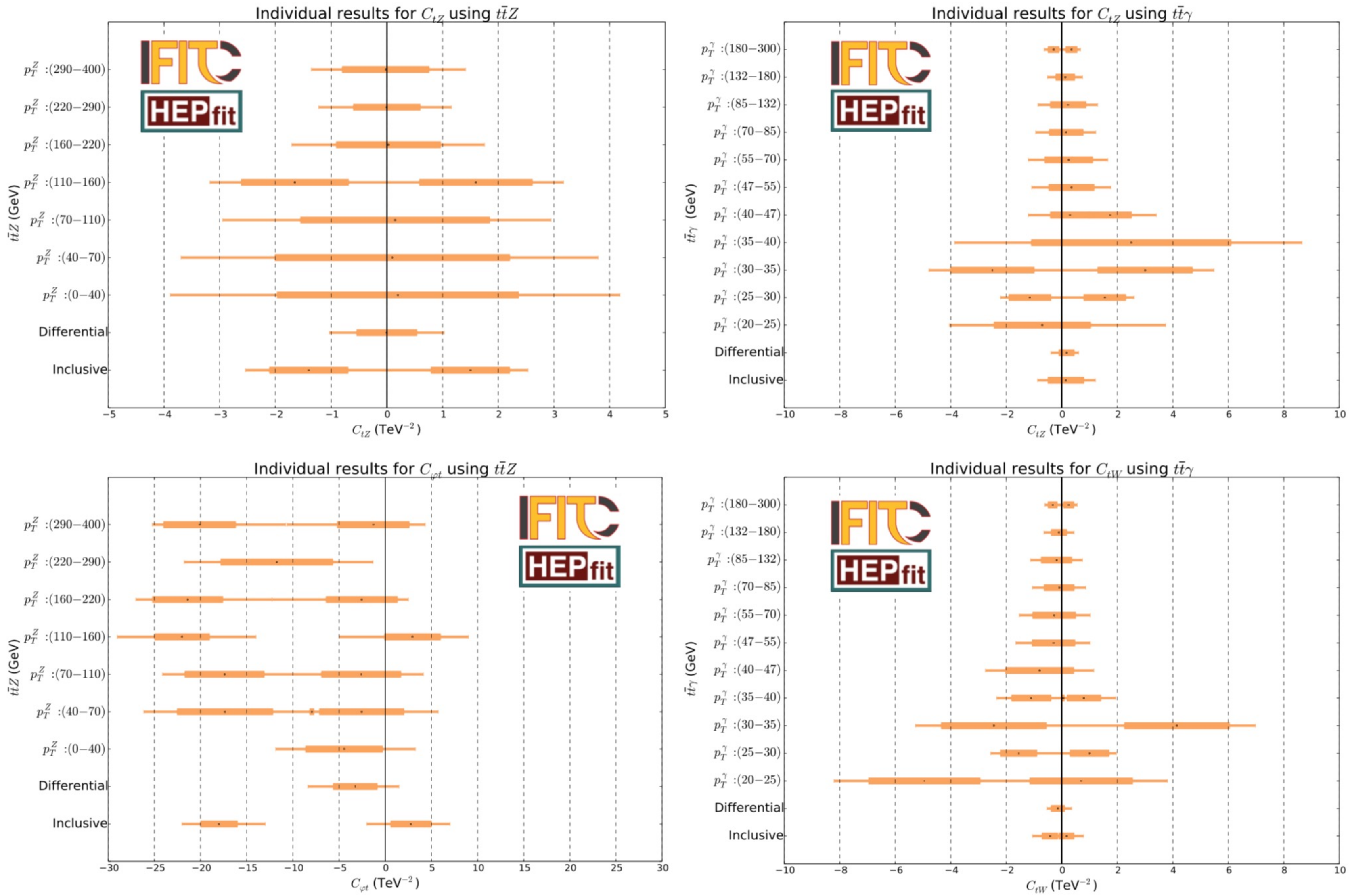

Results – Differential Cross Section Effect

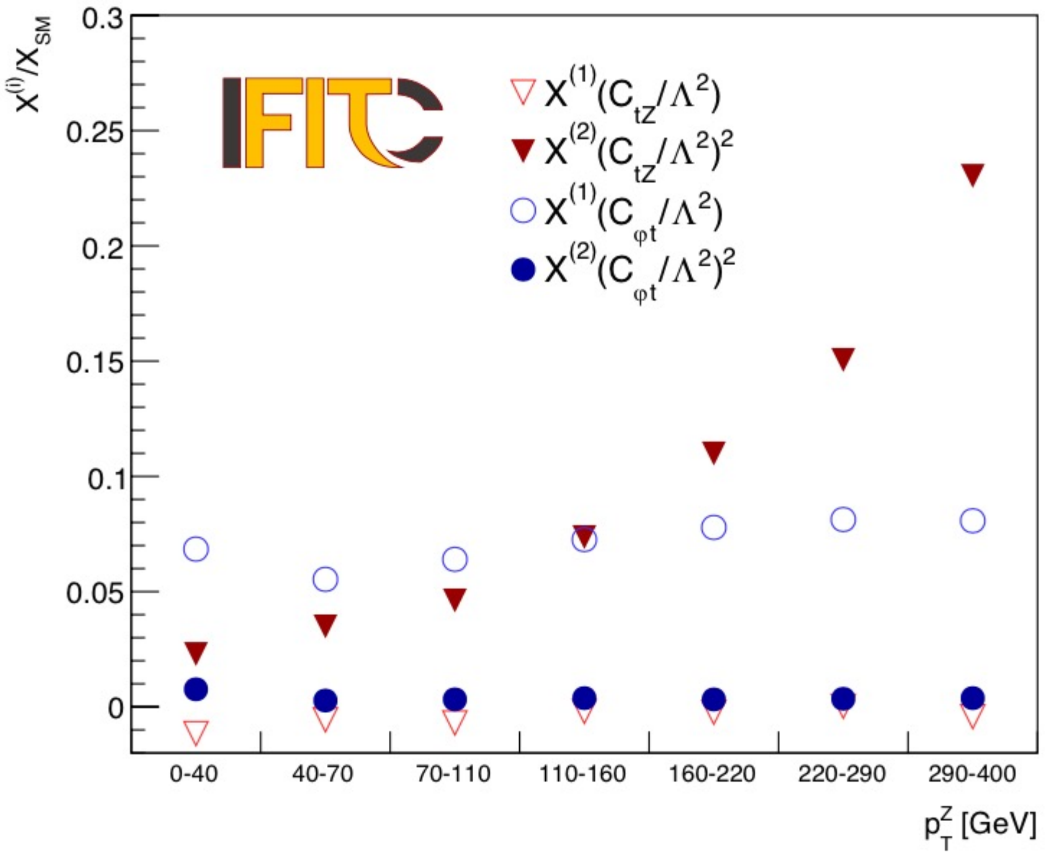

Figure 12. Linear and quadratic parameterisations for each of the bins in the differential ttZ cross-section. The two most sensitive operators to this process, C_{tZ} and $C_{\varphi t}$, are shown.

Results – Differential Cross Section Effect

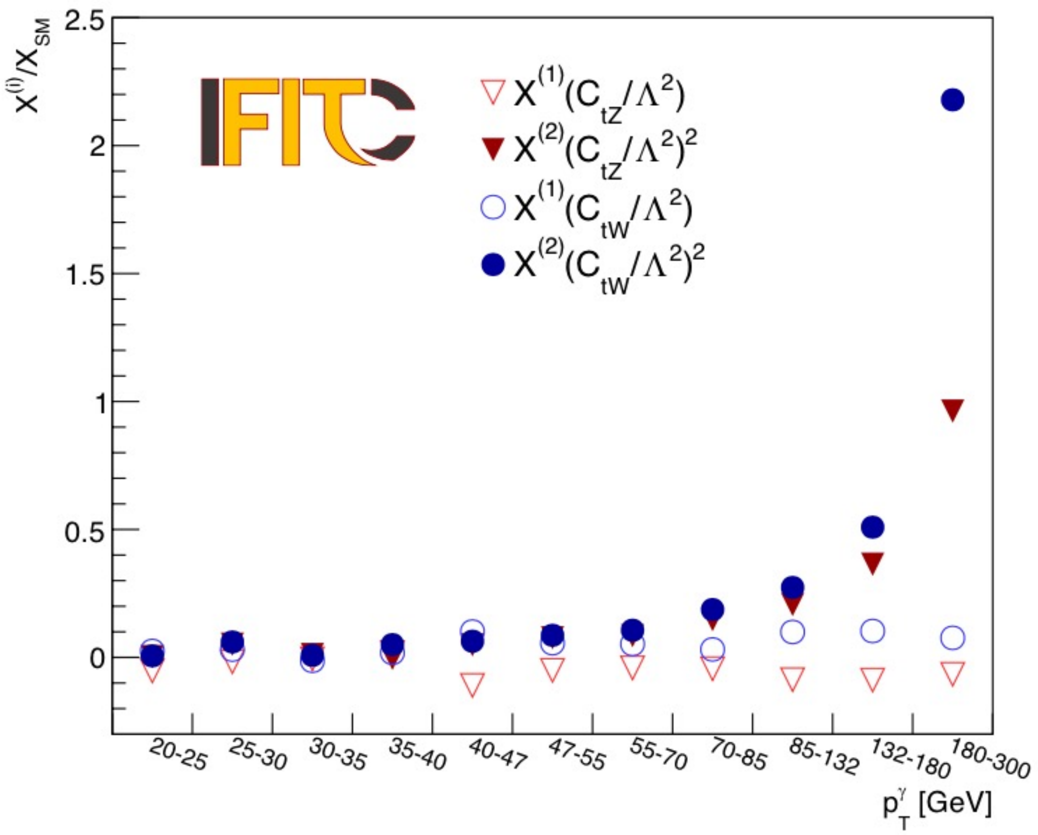

Figure 13. Linear and quadratic parameterisations for each of the bins in the differential $tt\gamma$ cross-section. The two most sensitive operators to this process, C_{tZ} and C_{tW}, are shown.

Complementarity btw. Observables

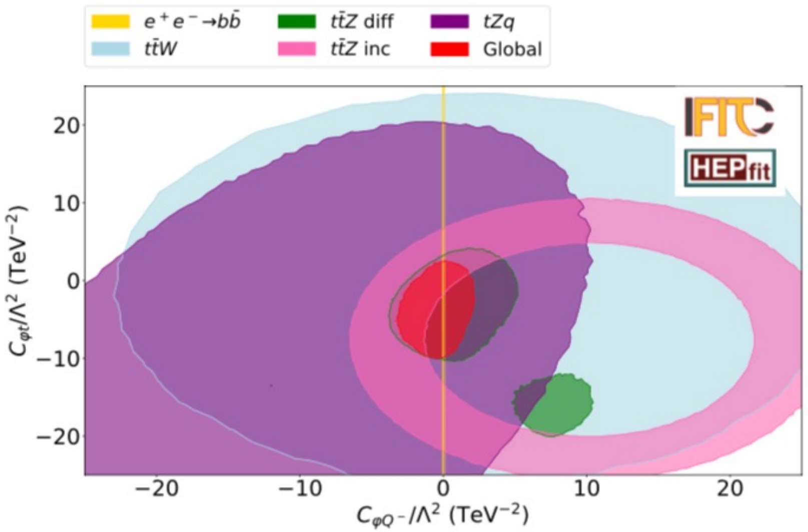

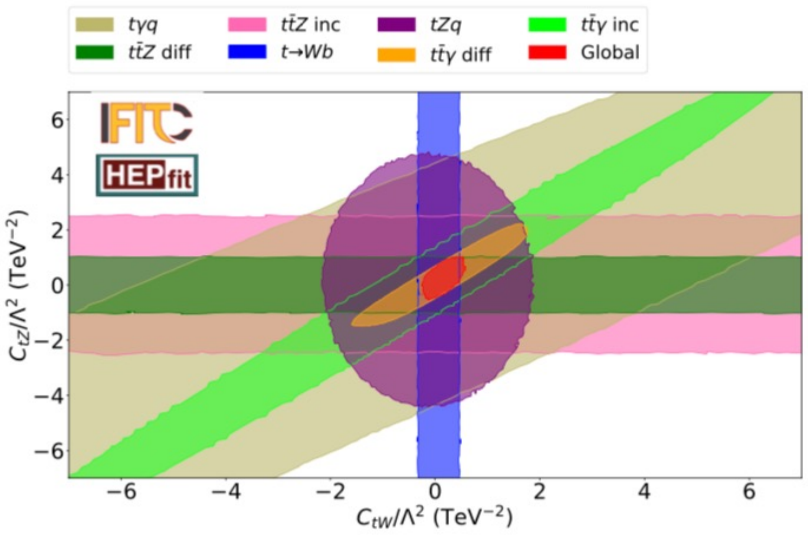

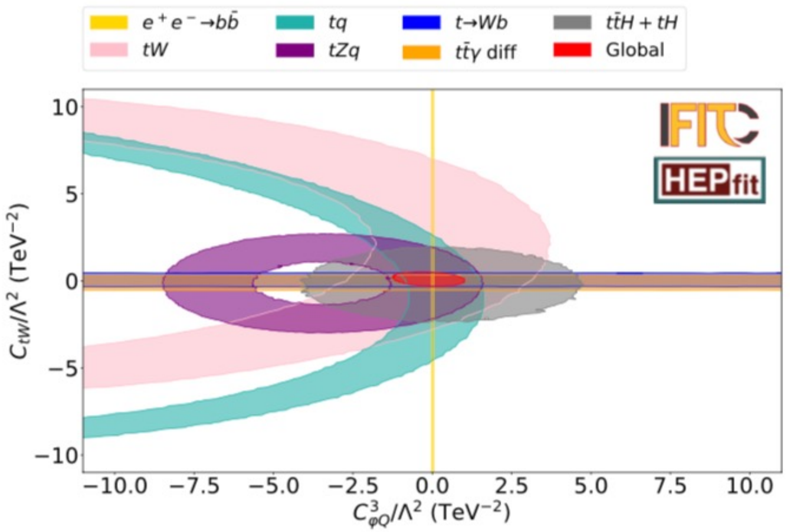

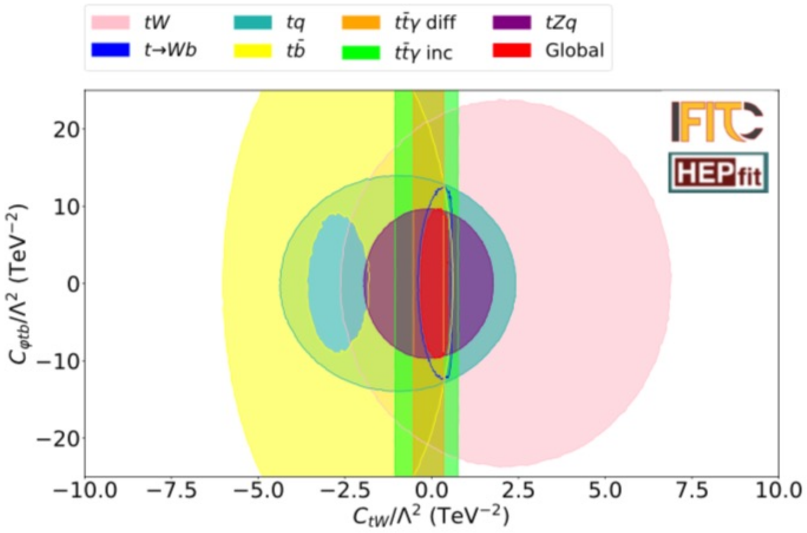

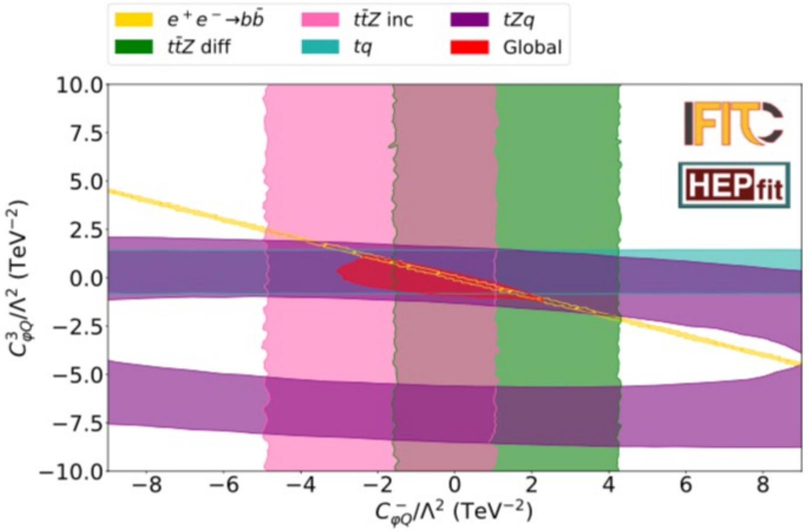

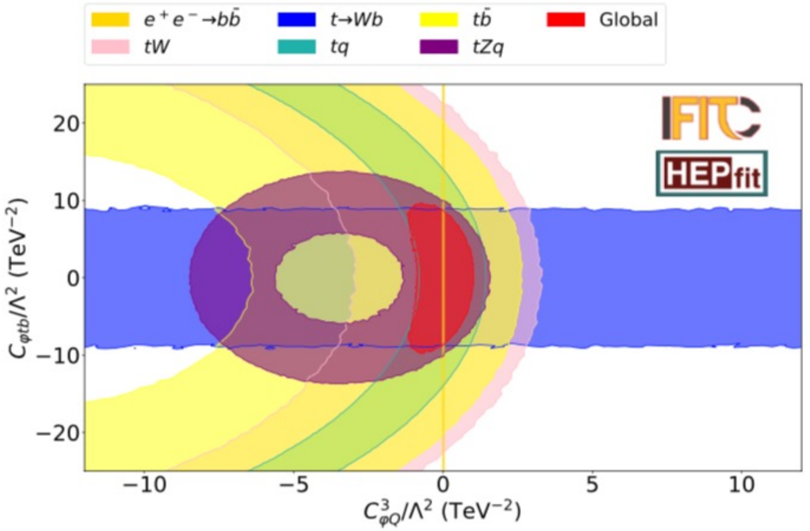

Limits on the Wilson Coefficients

C/Λ^2	Linear (95% probability)		Lin.+Quad. (95% probability)		(95% probability)
(TeV^{-2})	Individual	Global-Baseline	Individual	Global-Baseline	Global-Robust
$C_{t\varphi}$	[-3.17, 3.47]	[-3.13, 3.63]	[-3.05, 4.05]	[-2.82, 4.92]	[-121.82, 62.82]
$C^{-}_{\varphi Q}$	[-0.038, 0.079]	[-2.84, 0.78]	[-0.038, 0.079]	[-2.42, 1.62]	[-2.84, 1.62]
$C^{3}_{\varphi Q}$	[-0.019, 0.040]	[-0.41, 1.39]	[-0.019, 0.040]	[-0.94, 0.81]	[-0.94, 1.39]
$C_{\varphi t}$	[-6.6, 1.8]	[-8.96, 0.96]	[-8.6, 1.5]	[-9.01, 1.11]	[-37.50, 21.50]
C_{tW}	[-0.30, 0.38]	[-0.26, 0.44]	[-0.28, 0.32]	[-0.19, 0.50]	[-0.35, 0.50]
C_{tZ}	[-0.82, 2.21]	[-0.75, 2.37]	[-0.39, 0.57]	[-0.35, 0.88]	[-2.43, 3.53]
$C_{\varphi tb}$	–	–	[-6.61, 6.71]	[-7.55, 7.05]	–
C_{bW}	–	–	[-0.47, 0.47]	[-0.91, 0.91]	–

Table 2. Allowed ranges of the Wilson coefficients with a probability of 95% expressed in TeV^{-2} including only linear terms or linear and quadratic terms. We show, from left to right, the results of five fits: individual with linear terms, global baseline with linear terms, individual with linear and quadratic terms, global baseline with linear and quadratic terms and global robust limits. The robust result accounts for the effects of the correlations between the observables, the inclusion of further operators and the theoretical uncertainties on the parameterisations.

Experimental Correlations

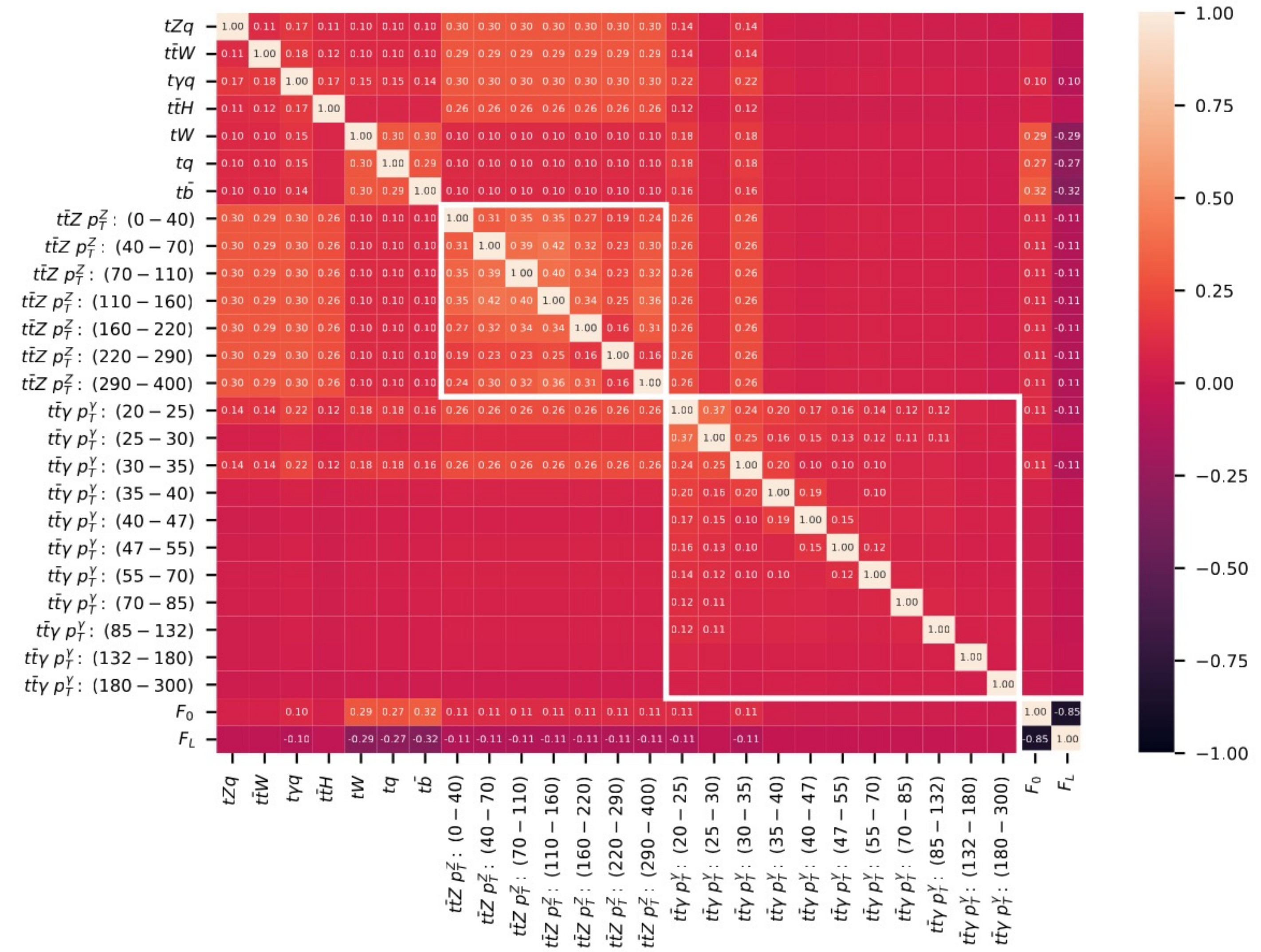

Figure 5. Experimental correlation matrix used. The boxes in white correspond to the correlations published by the experiments for $t\bar{t}Z$, $t\bar{t}\gamma$ and W boson helicity fractions [30, 33, 44]. The rest of the entries correspond to our ansatz, as described in Section 8.3. Cells are filled if the correlation is higher than 10% in absolute value.

Future Colliders – Uncertainties

Inclusive cross sections and helicities

Process	Measured (fb)	SM (fb)	LHC Unc.					HL-LHC Unc.				
			theo.	exp.				theo.	exp.			
				stat.	sys.	mod.	tot.		stat.	sys.	mod.	tot.
$pp \to t\bar{t}H + tHq$	640	664.3	41.7	90	40	70.7	121.2	20.9	19.4	8.6	35.4	41.3
$pp \to t\bar{t}Z$	990	810.9	85.8	51.5	48.9	67.3	97.8	42.9	11.1	10.6	33.6	37.0
$pp \to t\bar{t}\gamma$	39.6	38.5	1.76	0.8	1.25	2.16	2.62	0.88	0.17	0.27	1.08	1.13
$pp \to tZq$	111	102	3.5	13.0	6.1	6.2	15.7	1.75	2.09	0.98	3.1	3.87
$pp \to t\gamma q$	115.7	81	4	17.1	21.1	21.1	34.4	2	1.9	2.3	10.6	11.0
$pp \to t\bar{t}W + \mathrm{EW}$	770	647.5	76.1	120	59.6	73.0	152.6	38.1	13.1	6.5	36.5	39.4
$pp \to t\bar{b}$ (s-ch)	4900	5610	220	784	936	790	1454	110	35	42	395	399
$pp \to tW$	23100	22370	1570	1086	2000	2773	3587	785	49	89	1386	1390
$pp \to tq$ (t-ch)	87700	84200	250	1140	3128	4766	5810	125	51	140	2383	2390
F_0	0.693	0.687	0.005	0.009	0.006	0.009	0.014	0.003	0.0004	0.0003	0.004	0.004
F_L	0.315	0.311	0.005	0.006	0.003	0.008	0.011	0.003	0.0003	0.0002	0.004	0.004

Table: The data shown is the inclusive cross-section written in fb for all the channels except, obviously, for the W Helicities (F_0 and F_L).

Future Colliders – Uncertainties

$pp \to t\bar{t}Z$ differential cross section

$pp \to t\bar{t}Z$	Measured ($\text{fb} \cdot \text{GeV}^{-1}$)	SM ($\text{fb} \cdot \text{GeV}^{-1}$)	LHC Unc.					HL-LHC Unc.				
			theo.	exp.				theo.	exp.			
				stat.	sys.	mod.	tot.		stat.	sys.	mod.	tot.
p_T^Z : (0-40)	1.47	2.21	0.263	0.53	0.23	0.21	0.615	0.132	0.114	0.050	0.105	0.163
p_T^Z : (40-70)	4.32	4.59	0.543	0.94	0.60	0.51	1.223	0.272	0.203	0.130	0.253	0.349
p_T^Z : (70-110)	4.24	4.60	0.555	0.75	0.54	0.36	0.993	0.278	0.162	0.117	0.182	0.270
p_T^Z : (110-160)	4.4	3.45	0.429	0.55	0.43	0.39	0.800	0.215	0.118	0.093	0.197	0.248
p_T^Z : (160-220)	1.75	2.05	0.261	0.31	0.15	0.13	0.371	0.131	0.067	0.033	0.066	0.100
p_T^Z : (220-290)	0.58	1.03	0.130	0.16	0.047	0.034	0.174	0.065	0.035	0.010	0.017	0.041
p_T^Z : (290-400)	0.56	0.59	0.071	0.11	0.055	0.057	0.132	0.036	0.023	0.012	0.029	0.038

Table: We show the unfolded bin contents for the absolute parton-level differential cross-section measurement.

Future Colliders – Uncertainties

$pp \to t\bar{t}\gamma$ differential cross section

$pp \to t\bar{t}\gamma$	Measured ($\text{fb} \cdot \text{GeV}^{-1}$)	SM ($\text{fb} \cdot \text{GeV}^{-1}$)	LHC Unc.					HL-LHC Unc.				
			theo.	exp.				theo.	exp.			
				stat.	sys.	mod.	tot.		stat.	sys.	mod.	tot.
p_T^γ : (20-25)	1.782	1.670	0.066	0.116	0.168	0.108	0.231	0.033	0.025	0.036	0.054	0.070
p_T^γ : (25-30)	1.328	1.183	0.040	0.089	0.052	0.092	0.138	0.020	0.019	0.011	0.046	0.051
p_T^γ : (30-35)	0.966	0.8663	0.0302	0.072	0.026	0.060	0.097	0.0151	0.016	0.0056	0.030	0.0342
p_T^γ : (35-40)	0.705	0.6616	0.0205	0.058	0.015	0.042	0.0733	0.0103	0.0125	0.0032	0.021	0.0248
p_T^γ : (40-47)	0.474	0.4790	0.0160	0.04	0.0096	0.048	0.0629	0.0080	0.0086	0.0021	0.024	0.0254
p_T^γ : (47-55)	0.333	0.3464	0.0094	0.031	0.0067	0.017	0.0360	0.0047	0.0067	0.0014	0.0085	0.0109
p_T^γ : (55-70)	0.221	0.2188	0.0056	0.019	0.0038	0.0081	0.0210	0.0028	0.0041	0.00082	0.0041	0.0058
p_T^γ : (70-85)	0.122	0.1286	0.0031	0.014	0.0026	0.0069	0.0158	0.0016	0.0030	0.00056	0.0035	0.0046
p_T^γ : (85-132)	0.060	0.06037	0.0017	0.005	0.0014	0.0068	0.0086	0.00084	0.0011	0.00029	0.0034	0.0036
p_T^γ : (132-180)	0.020	0.02373	0.00077	0.003	0.00044	0.00080	0.00314	0.00039	0.00065	0.000095	0.00040	0.00077
p_T^γ : (180-300)	0.009	0.00790	0.00028	0.00045	0.000085	0.0014	0.00144	0.00014	0.000097	0.000018	0.00068	0.00069

Table: We show the unfolded bin contents for the absolute parton-level differential cross-section measurement.